

# Shear-Wave Splitting Indicates Non-Linear Dynamic Deformation in the Crust and Upper Mantle

Stuart Crampin, Gulten Polat, Yuan Gao, David B. Taylor,  
and Nurcan Meral Ozel

**Abstract** We demonstrate that non-linear dynamic deformation exists throughout the crust and upper mantle of the Earth. Stress-aligned shear-wave splitting, seismic birefringence, is widely observed in the Earth's upper crust, lower-crust, and uppermost ~400 km of the mantle. Attributed to the effects of pervasive distributions of stress-aligned fluid-saturated microcracks in the crust (and controversially intergranular films of hydrated melt in the mantle), the degree splitting indicates that 'microcracks' are so closely spaced that they verge on failure in fracturing and earthquakes if there is any disturbance. Phenomena that verge on failure are critical systems with non-linear dynamics that impose a range of new properties on conventional sub-critical geophysics that we suggest is a *New Geophysics*. Consequently, shear-wave splitting provides directly interpretable information about the progress of non-linear dynamic deformation in the deep otherwise-inaccessible interior of the microcracked Earth. Possibly uniquely for non-linear dynamic phenomena, observation of shear-wave splitting allows the progress towards singularities to be monitored in deep in situ rock, so that earthquakes and volcanic eruptions can be predicted (we prefer *stress-forecast*). The response to other processes, such as hydraulic fracking, can be monitored, and in some cases calculated and effects predicted. Here, we review shear-wave splitting and demonstrate the prevalence of non-linear dynamic deformation of the New Geophysics in the crust and uppermost ~400 km of the mantle.

**Keywords** Monitoring fracking • *New Geophysics* • Non-linear dynamics • Shear-wave splitting • Stress-aligned microcracks • Stress-forecasting earthquakes • Stress-forecasting volcanic eruptions

---

## Preamble

Schopenhauer 1788–1860: 'All truth passes through three stages: ridicule; violent-opposition; self-evident'.

S. Crampin (✉) • G. Polat • Y. Gao • D.B. Taylor • N.M. Ozel  
British Geological Survey, The Lyell Centre, Edinburgh, EH14 4AP, Scotland, UK  
e-mail: scrampin@ed.ac.uk

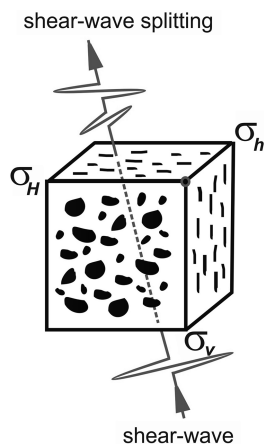
# 1 Introduction

Since Crampin et al. (1980), shear-wave splitting (SWS) has been widely observed with stress-aligned polarizations and  $\sim 1.5$  to  $\sim 4.5\%$  shear-wave velocity anisotropy (SWVA) throughout the upper- and lower-crust (Crampin 1994), reviewed by Crampin and Peacock (2008). Similarly, since Ando et al. (1980), SWS has been widely observed with nearly identical stress-aligned polarizations and SWVA, throughout the uppermost  $\sim 400$  km of the mantle, reviewed by Silver (1996) and Savage (1999).

The presence of SWS indicates some form of seismic anisotropy the effective elastic constants. The only anisotropic symmetry system that has the observed parallel SWS polarizations at a horizontal free-surface is hexagonal symmetry (transverse isotropy) with a horizontal axis of cylindrical symmetry (aka HTI-symmetry) (Crampin 1981; Crampin and Kirkwood 1981), and the only common geological phenomenon with HTI-symmetry is parallel vertical fluid-saturated microcracks. Hence the observed SWS at the surface indicates distributions of stress-aligned vertical fluid-saturated microcracks along almost all ray paths in the crust, and stress-aligned intergranular films of hydrated melt in the uppermost  $\sim 400$  km of the mantle (Crampin 2003). Figure 1 is a schematic dimensionless illustration of SWS throughout the microcracked crust and upper mantle, where the (realistically imaged) closely spaced microcracks indicate sufficient compliance for non-linear dynamic (NLD) deformation.

Here, we briefly review SWS (and the evidence for extensive NLD deformation) in the Earth's interior, and demonstrate that, possibly uniquely for NLD studies, the progress towards singularities (fracture criticality and earthquakes in geophysics) can be monitored by analysing SWS time delays. We outline several applications of NLD.

**Fig. 1** Schematic illustration of shear-wave splitting on propagation through the fluid-saturated stress-aligned microcracks pervasive in almost all rocks in the Earth's crust (after Crampin 1994)



2 A Review of Shear-Wave Splitting

Azimuthally varying SWS is widely observed throughout the crust and uppermost ~400 km of the mantle (Crampin et al. 1980; Crampin 1994; Silver 1996; Savage 1999; Crampin and Peacock 2008; Crampin and Gao 2013). The SWS is generally interpreted as propagation through distributions of stress-aligned fluid-saturated microcracks in the upper- and lower-crust, where the fluid is typically water (possibly supercritical at depth), and in the upper-mantle, where the fluid is (more controversially) intergranular films of hydrated melt (Crampin 2003; Crampin and Gao 2016). Since crack density  $\epsilon \approx \%SWVA/100$  (Hudson 1981), the range of observed SWVA implies crack densities of  $\epsilon \approx 0.015\text{--}0.045$  (Crampin 1994). Percolation theory indicates through-going fluid pathways at  $\epsilon \approx 0.055$  (Crampin and Zatsepin 1997a, b; Crampin 1999). Associating fracture-criticality with the percolation-threshold, if there is any disturbance microcracks will fail at fracture-criticality of  $\epsilon \approx 0.055$  ( $SWVA \approx 5.5\%$ ) (Crampin et al. 1999, 2008). Since SWVA of 1.5–4.5% is close to 5.5%, this implies that almost all in situ rocks throughout the crust and upper-mantle of the Earth verge on failure.

Figure 2 is a schematic illustration of crack distributions for a range of crack densities, where the two left-hand images are for observed SWS (Crampin 1994; Crampin and Gao 2013). Since phenomena verging on failure are critical-systems with NLD deformation. Observations of SWS indicate that much of the Earth above ~450 km depth has NLD deformation.

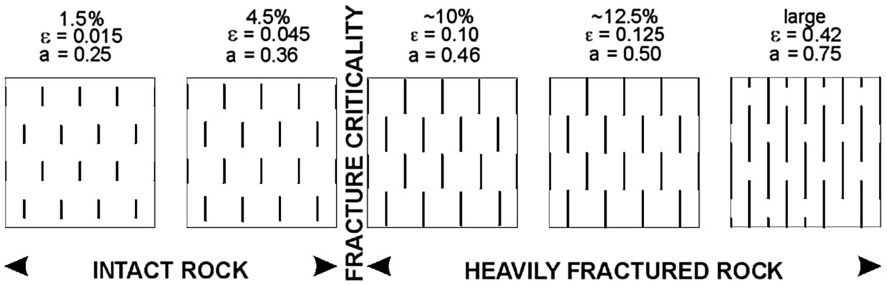
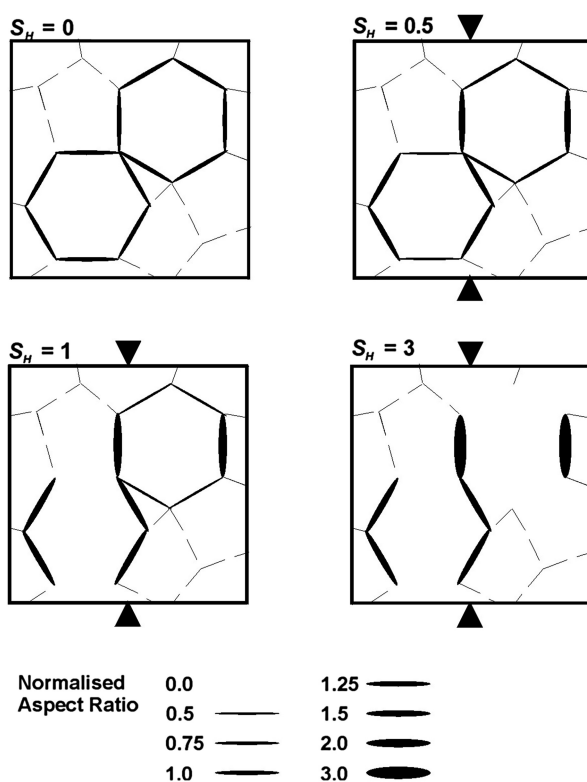


**Fig. 2** Schematic (dimensionless) illustration of the observed percentages of shear-wave velocity-anisotropy interpreted as uniform distributions of equal-sized parallel penny-shaped cracks, where  $\epsilon$  is crack density, and  $a$  is crack radius per unit cube. Images are 2D cross sections of 3D crack distributions. Fracture criticality is at the percolation threshold  $\epsilon = 0.055$  for stress-aligned microcracks, where cracks are so closely spaced they verge on fracturing if there is any disturbance (after Crampin 1994; Crampin and Zatsepin 1997a)

## 2.1 APE-Modelling

The suggested mechanism for low-level deformation is fluid-displacement by flow or dispersion between intergranular microcracks cracks at different orientations to the stress field in a process known as anisotropic poro-elasticity (APE) illustrated schematically in Fig. 3. Figure 3 shows APE-deformation of a dimensionless initially random distribution stress-aligned *vertical* cracks for four values of differential horizontal stress ( $s_H = 0.0, 0.5, 1.0, 3.0$ ). Hexagons are elastically isotropic (Crampin and Kirkwood 1981) so that, under zero differential (horizontal) stress ( $s_H = s_h = 0$ ) (top left) microcracks have equal aspect ratios (equal crack thicknesses), and the two solid hexagons are a small selection of randomly oriented vertical cracks with zero SWVA. Following a small increase in stress to  $s_H = 0.5$  (top right), cracks perpendicular to  $s_H$  have greater pressure normal to the cracks than cracks parallel to  $s_H$ , and fluid migrates by flow or dispersion along the pressure gradients between neighbouring microcracks at different orientations to the stress field. Some cracks swell (increase in aspect-ratio) and some cracks thin, but without crack closure there is no significant SWVA and the overall elasticity is still essentially isotropic. As differential stress increases, there is a critical point

**Fig. 3** Schematic (dimensionless, but spatially accurate), illustration of anisotropic poro-elasticity (APE) deformation of fluid-saturated microcracks. There is a more detailed description of the behaviour in Crampin (1999) (after Crampin 1999)



(normalized to  $s_H = 1$ ), when cracks normal to  $s_H$  to first begin to close (bottom left), and SWVA jumps from zero to a minimum of approximately  $\sim 1.5\%$  SWVA. This theoretical minimum is approximately the same as the minimum SWVA observed in the Earth, imaged in the left-hand diagram in Fig. 2, validating APE-deformation within the Earth (Crampin 1994). As  $s_H$  increases to  $s_H \approx 3$ , cracks begin to align (Fig. 3, bottom right), and at the percolation threshold at  $s_H \approx 5.5$  (not modelled), fracture-criticality is reached and the rock fractures if there is any disturbance (Crampin and Zatsepin 1997a, b).

Note that the NLD of APE-deformation as illustrated in Fig. 3 is dimensionless and valid for any 3D distributions of crack and stress geometries. Figure 3 shows APE-deformation illustrated only for vertical cracks because: (1) parallel cracks can be drawn in orthogonal 2D planar diagrams as in Fig. 3; and (2), once below the depth, where increasing vertical stress  $\sigma_V$  equals the minimum horizontal stress  $\sigma_h$ , microcracks in the Earth do tend to be vertical, parallel and normal to  $\sigma_h$ .

The key effect of APE-deformation in the NLD deformation imaged in Fig. 3 is that increasing differential stress increases the aspect ratio (makes cracks swell) of cracks aligned perpendicular to the direction of minimum tectonic stress  $s_h$ . The NLD deformation of stress-accumulation before earthquakes, say, can be monitored by measuring the increasing *average* SWS time-delay in Band-1 directions in the shear-wave window (Crampin 1999; Crampin et al. 2008; Crampin and Gao 2016). The shear-wave window and Band-1 and Band-2 directions are described in Fig. 5, Appendix 1.

## 2.2 Measuring SWS Parameters on Seismograms

Various techniques have been used to automatically measure the polarizations ( $\Phi$ ) and time-delays ( $dt$ ) of SWS on shear-wave seismograms. The results are generally unsatisfactory. The problem is that SWS, although simple in principle, in practice may be extremely complicated for seismograms in the crust, and it is difficult to assess the reliability of fully automated techniques (Crampin 2006). The preferred technique uses the semi-automatic Shear-Wave Analysis System (SWAS) for measuring shear-wave splitting parameters, where reliability of the results for each arrival displayed in 2D polarization diagrams is easy to visually assess (Hao et al. 2008). We show a typical example in Fig. 4 where SWAS is applied to a small  $M = 1.43$  earthquake in SW Iceland.

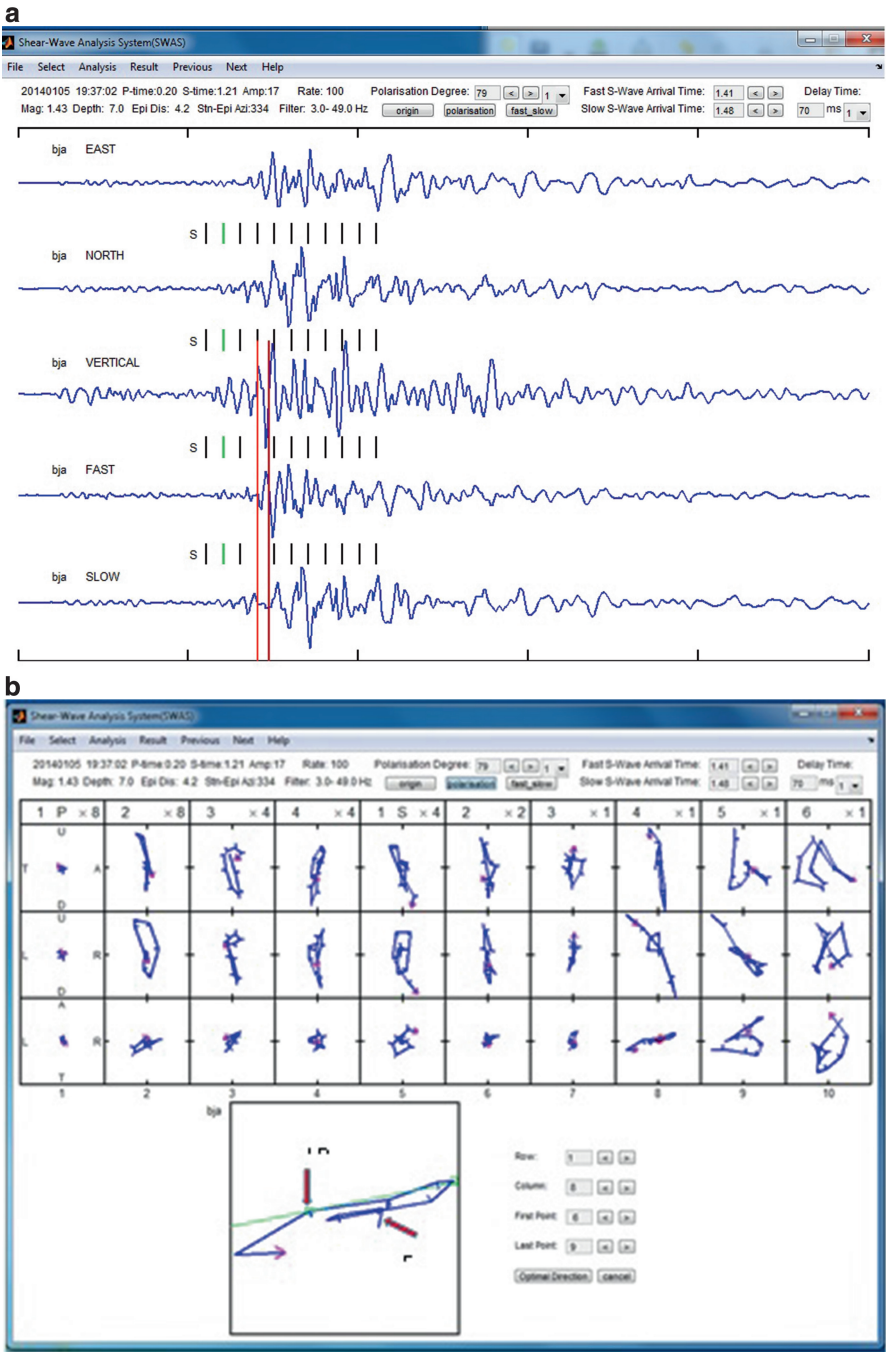


Fig. 4 (continued)

### 2.3 *Shear-Wave Splitting (SWS) and Non-Linear Dynamic Deformation in the Earth*

SWS is widely observed throughout the crust and uppermost  $\sim 400$  km of the mantle with the configuration of Fig. 2 (Crampin and Peacock 2008) with the implied deformation of Fig. 3, which is clearly NLD deformation if there is any disturbance. This means that NLD deformation is prevalent throughout the crust and upper mantle of the Earth.

## 3 The New Geophysics

The NLD effects of APE-deformation are widely observed in extensive observations if SWS and imply a *New Geophysics* of wave propagation in critically microcracked rock with effects and properties that cannot be matched in conventional sub-critical geophysics without innumerable special cases (Crampin and Gao 2013). Table 1 lists observations of 19 different phenomena some along thousands to millions of shear-wave ray-paths (in industrial seismic-exploration), which match the effects of APE and support the critical New Geophysics. The list could easily be extended. This means that NLD deformation and New Geophysics are established throughout the crust and uppermost  $\sim 400$  km of the mantle. There are no contrary observations known to us.

Seismic-wave propagation in such NLD critical-systems is necessarily different from wave propagation in conventional sub-critical geophysics and imposes the range of fundamentally new properties on sub-critical geophysics listed in Table 2. These new properties allow several new applications.

NLD is confirmed by the new properties of the *New Geophysics* of critical-systems of distributions of stress-aligned fluid-saturated microcracks that are not available in conventional sub-critical geophysics. With one exception the new properties in Table 2 have all been recognized in the Earth in some cases, thousands to millions of times, in oil company reflection seismics and other circumstances; however, these ideas are innovative and remain controversial (the Preamble is apposite). The exception, controllability, has not yet been tested. Observations of these prop-



**Fig. 4** Example of SWS measurements using SWAS (Hao et al. 2008). (a) Seismograms of small  $M = 1.43$  earthquake recorded at station BJA in SW Iceland in recording geometry East, North, Vertical and rotated into orthogonal Fast and Slow shear-wave polarizations. *Red lines* mark the Fast and Slow SWS arrivals—note ‘quiet’ segment (the SWS time-delay,  $dt$ ) between the *red lines* in the slow direction. (b) 3D polarization diagrams in the time intervals in (a) in directions (U)p, (D)own, and (T)owards, (A)way, and (L)eft and (R)ight from the source, with enlarged diagram showing semi-automated picks of fast (F) and slow (S) arrivals, where for illustration they are identified by manually positioned *arrows*. The Fast polarization is automatically picked in *green*

**Table 1** Evidence for NLD supporting APE-deformation and the critical New Geophysics (Crampin and Gao 2013)

Evidence inexplicable in terms of conventional sub-critical geophysics <sup>a</sup>	
(1)	Shear-wave splitting is observed in almost all in situ rocks in the crust and upper mantle (Crampin 1994, 1999; Crampin and Peacock 2008; Crampin and Zatsepin 1997a)
(2)	There is a minimum shear-wave velocity anisotropy (SWVA) of $\sim 1.5\%$ in almost all in situ rocks (Crampin 1994, 1999; Crampin and Peacock 2008; Crampin and Zatsepin 1997a)
(3)	There is a maximum SWVA of $\sim 5.5\%$ in ostensibly unfractured rock (Crampin 1994, 1999; Crampin and Peacock 2008; Crampin and Zatsepin 1997a)
(4)	Fracture-criticality limit of SWVA is $\sim 5.5\%$ in in situ rocks independent of rock-type, geology, tectonics, and porosity, etc., where SWVA of $\sim 5.5\%$ is the percolation threshold for parallel cracks (Crampin 1994, 1999; Crampin and Peacock 2008; Crampin and Zatsepin 1997a)
(5)	High pore-fluid pressures induce $90^\circ$ -flips in polarizations of the faster split shear-waves (Angerer et al. 2002; Crampin et al. 2002)
(6)	Explains the large ( $\pm 80\%$ ) scatter in shear-wave time-delays above small earthquakes (Crampin et al. 2002; Crampin et al. 2004b)
(7)	Effects of $\text{CO}_2$ -injections on seismic reflection surveys modelled by APE (Angerer et al. 2002; Crampin et al. 2002; Crampin et al. 2004b)
(8)	Stress-accumulation observed before earthquakes (Volti and Crampin 2003b; Crampin et al. 1999; Crampin et al. 2008)
(9)	Time, magnitude and impending fault-break successfully stress-forecast in real time (Crampin et al. 1999; Crampin et al. 2008)
(10)	Stress-relaxation (crack-coalescence) observed before earthquakes (Crampin and Peacock 2008; Gao and Crampin 2004)
(11)	Stress-accumulation observed before volcanic eruptions (Crampin and Peacock 2008; Volti and Crampin 2003b; Crampin et al. 1999)
(12)	Extreme sensitivity: stress-variations observed in Iceland two and a half years before the Sumatra-Andaman EQ at the width of the Eurasian Plate from Indonesia (Crampin and Gao 2012)
(13)	Explains how a stressed rock differs from an unstressed rock
(14)	Explains how the enormous stress-energy before a large earthquake accumulates without inducing smaller earthquakes (Crampin et al. 2013)
(15)	Explains why initial stress drop at an earthquake is small (typically 2–4 MPa) and independent of earthquake magnitudes which may vary by over ten orders of magnitude (Crampin et al. 2013)
(16)	Explains how irregular fault-planes slip when constrained by enormous lithostatic stress (Crampin et al. 2013)
(17)	Explains why we cannot deterministically predict but can stress-forecast the time, magnitude and fault-break of impending earthquakes (Crampin et al. 2013)
(18)	Explains why the Gutenberg and Richter (1956) relationship between logarithms of cumulative frequencies of earthquakes and earthquake magnitudes is linear (Crampin et al. 2013)
(19)	Partly explains why, despite huge investments, average recovery is less than 40% of in-place oil (Crampin 2006)

<sup>a</sup>Without innumerable special cases

**Table 2** Properties of *New Geophysics* of NLD in compliant critically microcracked in situ rock (after Crampin and Gao (2013))

(1)	Self-similarity:	Logarithmic plots of many properties are linear, such as Gutenberg-Richter relationship (Gutenberg and Richter 1956; Gao and Crampin 2004)
(2)	Monitorability:	Behaviour can be monitored with SWS (Crampin 1999; Crampin and Peacock 2005; Crampin and Peacock 2008)
(3)	Uniformity:	Statistical behaviour is more like other critical systems than it is to the underlying sub-critical physics (Crampin and Peacock 2005; Crampin and Peacock 2008)
(4)	Calculability:	Behaviour is more uniform (universal) than sub-critical behaviour and can be modelled or calculated with the equations of Anisotropic Poro-Elasticity, APE (Crampin and Peacock 2008; Angerer et al. 2002; Crampin and Zatsepin 1997a, b)
(5)	Predictability:	If impending changes can be quantified, behaviour can be predicted by APE (Crampin and Peacock 2008; Angerer et al. 2002; Crampin and Zatsepin 1997a, b)
(6)	Controllability:	If conditions can be monitored (Item 2), calculated (Item 4) and modified by injection pressures (Crampin and Peacock 2008; Angerer et al. 2002), in principle the behaviour of the in situ rock mass can be controlled by feedback (optimizing flow-directions by fluid-injection, say, in hydrocarbon production)
(7)	Universality:	Effects pervade all available space (Crampin and Gao 2013; Volfi and Crampin 2003a, b; Crampin and Gao 2012)
(8)	Sensitivity:	Butterfly wings effect sensitivity to miniscule differences in initial conditions (Volfi and Crampin 2003a, b; Crampin and Gao 2012)

erties of SWS allow us to monitor the approach of singularities in the interior of the medium to be monitored in detail. This property is believed to be unique in NLD and leads to several important applications. Three definitive applications, verifying NLD and New Geophysics, are briefly outlined in the Appendices: Appendix 2—stress-forecasting (predicting) earthquakes; Appendix 3—stress-forecasting (predicting) volcanic episodes; and Appendix 4—determining the response of a reservoir to critical and sub-critical fluid CO<sub>2</sub>-injections (hydraulic fracking). These appendices are brief summaries, and more complete discussions are in the references.

## 4 Conclusions

We have shown that seismic shear-wave splitting monitors the non-linear dynamic deformation of the crust and uppermost ~400 km of the mantle. Deformation is by fluid movement by flow or dispersion between critical-systems of neighbouring ‘microcracks’ in the crust, and intergranular films of hydrolyzed melt in the mantle at different orientations to the stress-field. This can be imaged by anisotropic poro-elastic (APE) deformation of the stress-aligned fluid-saturated microcracks pervading almost all in situ rock. This behaviour has been classed as a New Geophysics and imposes many fundamentally new properties on conventional sub-critical geophysics and opens new applications for geophysics.

Table 3 lists proven and potential applications of NLD deformation. These ideas are controversial (see Preamble) and difficult to get funded; hence, only three applications have currently been explored: stress-forecasting/predicting earthquakes (Appendix 2); stress-forecasting/predicting volcanic eruptions/episodes (Appendix 3); and modelling, calculating, and predicting the effects of fluid-injections (aka hydraulic fracking) (Appendix 4). Table 3 also lists other potential industrial and societal applications.

We conclude that the NLD deformation of New Geophysics exists throughout the crust and uppermost ~400 km of the mantle and has a number of possibly important proven and potential applications.

**Table 3** Potential applications of NLD and SWS in the New Geophysics

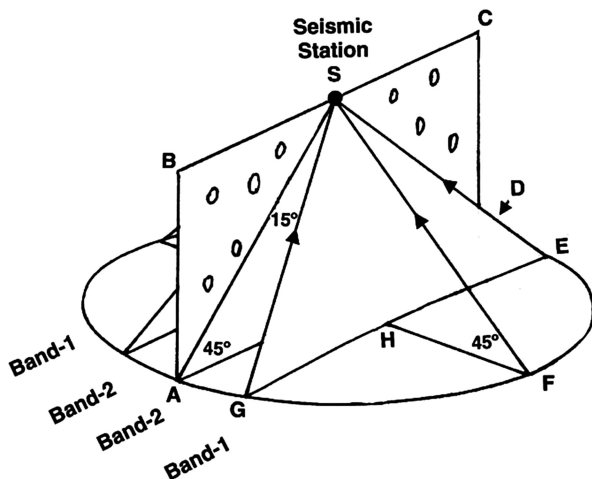
<i>Proven applications</i>
(1) Using SWS for stress-forecasting/predicting impending earthquakes (Appendix 2; Crampin and Gao 2013)
(2) Using SWS for stress-forecasting/predicting impending volcanic eruptions (Appendix 2; Volti and Crampin 2003b)
(3) Using APE to monitor, calculate, predict hydraulic injection (hydraulic fracking) (Appendix 3; Angerer et al. 2002)
<i>Potential applications in hydrocarbon recovery</i>
(4) SWI: monitoring production with time-lapse seismics in Single-Well Imaging (Crampin and Gao 2013)
(5) SMORE: Slower production for More Oil REcovery (Crampin and Gao 2013)
(6) OWF: optimizing water-flooding with APE-modelling and feedback (Crampin and Gao 2013)
<i>Other potential applications</i>
(7) Monitoring seismic security of vulnerable locations: cities, nuclear power stations, dams, etc. (Crampin and Gao 2013)
(8) Monitoring, calculating and predicting the response of a reservoir to CO <sub>2</sub> sequestration (Crampin and Gao 2013)
(9) Monitoring nuclear waste deposition with an adjacent borehole stress-monitoring site (SMSs) (Crampin and Gao 2013)
(10) Monitoring rock failure in mining, landslides, tunnelling, etc. by adjacent SMSs (Crampin and Gao 2013)

**Acknowledgements** The authors thank Sheila Peacock and Peter Leary for their comments. Yuan Gao was partially supported by the National Natural Science Foundation of China, Project 41174042. We thank the Director of Science and Technology of the British Geological Survey (NERC) for approval to publish this paper.

## Appendix 1: Ray-Path Geometry for Observing Undisturbed Shear Waves and SWS at the Shear-Wave Window at a Horizontal Free-Surface, and Identification of Band-1 and Band-2 Directions in Distributions of Parallel Vertical Fluid-Saturated Microcracks

Figure 5 shows ray-path geometry for observing undisturbed waveforms of *SV*-waves and SWS in stress-aligned fluid-saturated microcracks in the effective shear-wave window at a horizontal free-surface. (The wave-forms of *SH*-waves are preserved for all angles of incidence at a horizontal free-surface.) ABSCD is the crack-plane through distributions of parallel-vertical microcracks, and S is the recorder on a horizontal free-surface. The exact shear-wave window in an isotropic half-space is ray paths within the solid angle subtending  $\sin^{-1}(V_s/V_p) \approx 35^\circ$  marking the critical angle for *V<sub>p</sub>* reflection (Booth and Crampin 1985). The effective

**Fig. 5** Ray-path geometry for observing undisturbed waveforms of shear-waves and SWS in stress-aligned fluid-saturated microcracks in the shear-wave window at a horizontal free-surface (after Crampin and Gao 2013)



shear-wave window is ray paths within the solid angle AGFED-to-S and similar ray paths reflected in the crack-plane. However, near-surface low-velocity layers in the Earth bend rays upwards so that the effective shear-wave window may often be taken as straight-line ray paths out to  $45^\circ$  as in Fig. 5.

Band-1 directions to the free-surface, where time-delays are sensitive to crack aspect-ratio (Crampin 1999; Crampin and Gao 2016), are within the solid angle EFGH-to-S subtending  $15\text{--}45^\circ$  to the crack plane within the effective shear-wave window. Band-2 directions to the free-surface, where time-delays are dominated by crack-density (Crampin 1999), are within the solid angle ADEHG-to-S to the crack plane. Both Band-1 and Band-2 directions include equivalent solid-angle directions reflected in the far side of the imaged crack plane (After Crampin and Gao 2013).

## Appendix 2: Monitoring NLD Deformation to Stress-Forecast Impending Earthquakes

The effects of changing stress on in situ rocks can be monitored by SWS imaging NLD changes in microcrack geometry (Crampin 1999; Crampin and Peacock 2008; Crampin and Gao 2016). Observations of SWS indicate that increases of stress in the Earth (typically originate from magma generation and subduction, and interactions at the margins of tectonic plates) can be monitored by measuring changes in SWS. Initially, such NLD stress-accumulation is widespread throughout tectonic plates and the stress-field does not initially identify the fault-planes where the stress will eventually be released by slippage in earthquakes. The accumulating stress modifies crack aspect ratios throughout the stressed rock-mass, until the microcrack geometry approaches levels of fracture-criticality (Crampin 1999). Only then does the stress-

field concentrate on envelopes of weakness surrounding the impending fault-planes, and stress-relaxation occurs as microcracks coalesce onto the impending fault break in NLD deformation (Gao and Crampin 2004; Wu et al. 2006; Crampin and Peacock 2008; Crampin and Gao 2013; Crampin et al. 2013).

The Earth is highly heterogeneous and stress accumulates irregularly. If stress accumulates over a small rock volume, the increase will be rapid but the eventual earthquake will be small. If stress accumulates over a larger volume, the increase will be slower but the eventual earthquake will be larger. Consequently, durations of the changes and the magnitudes possess self-similarity, so that monitoring NLD changes in the surrounding rock mass allows the time, magnitude, and in some cases fault break, of the impending earthquake to be stress-forecast. Note that we refer to this phenomenon as *earthquake stress-forecasting*, rather than *earthquake forecasting* or *earthquake prediction*, to emphasize the different methodology.

New Geophysics demonstrates that stress-accumulation before earthquakes can be recognized by increasing *average* SWS time-delays in *Band-1* directions in the shear-wave window (Fig. 5), and corresponding decreases in *average* SWS time-delays for stress-relaxation (Crampin 1999; Crampin and Peacock 2008; Crampin and Gao 2013, 2016). NLD stress-accumulation was first positively identified in changes in SWS before a  $M$  5 earthquake in Iceland with similar changes in SWS to those before a  $M$  5.1 earthquake 6 months earlier (Fig. 6). A stress-forecast was emailed (10th Nov., 1998) to the Iceland Meteorological Office (IMO) ‘... an event could occur any time between now ( $M \geq 5$ ) and the end of February ( $M \geq 6$ )’ on a specified fault with continuing seismic activity. Three days later (13th Nov., 1998), a  $M = 5$  earthquake occurred on the identified fault (Crampin et al. 1999, 2004a, 2008). We claim this as the first successful scientifically stress-forecast/predicted earthquake, as opposed to less-specific probabilistic estimates. Similar characteristic variations are seen retrospectively before 16 earthquakes elsewhere (Crampin and Gao 2015).

Later, it was recognized that the observed stress-accumulation stops abruptly before the impending earthquake occurs. There is stress-relaxation, average time-delays decrease, and the earthquake occurs at a comparatively low value of implied stress (Gao and Crampin 2004). Figure 7 shows stress-accumulation and stress-relaxation, before six earthquakes (and two laboratory experiments) ranging in magnitude from  $M$  6 to  $M$  1.7, in a normalized format convenient for displaying such characteristic changes. The successfully stress-forecast earthquake is Fig. 7c. All six earthquakes show similar behaviour despite orders of magnitude differences in released energy and durations of stress-accumulation ranging from 6 years to a few hours.

Logarithms of the durations of both the stress-accumulations and the stress-relaxations are both linear (self-similar) with the impending magnitudes (Crampin et al. 1999, 2008; Gao and Crampin 2004; Crampin and Peacock 2008). Stress-relaxation is interpreted as microcracks coalescing onto the impending fault-plane (Gao and Crampin 2004; Wu et al. 2006). Characteristic patterns of stress-accumulation increases and stress-relaxation (crack-coalescent) decreases have been recognized retrospectively before (currently) 15 earthquakes ranging from a  $M$  1.7

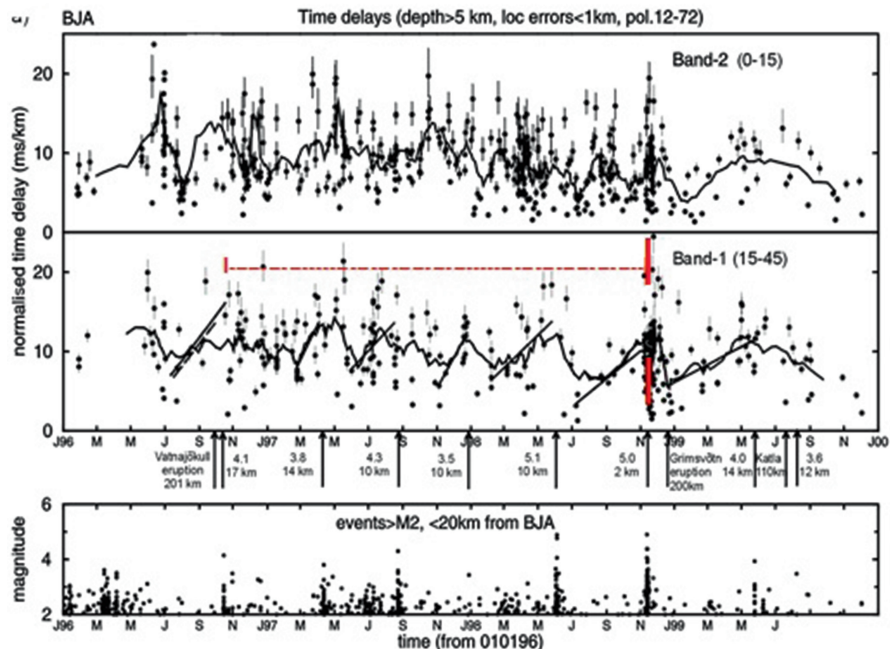


**Fig. 6** Variations with time of SWS time-delays normalized to ms/km in Band-1 directions (*middle diagram*) and Band-2 directions (*Top diagram*) for 5 years at station BJA in SW Iceland showing, in Band-1, least-squares increases before larger earthquakes within 20 km of BJA in *lower diagram*. The curves in the time-delays in the *top* and *middle* diagrams are nine-point moving averages. The *red line* (Oct. 1996–Nov. 1998) marks a least-squares average of 2 ms/km/year relaxation interpreted as the Mid-Atlantic Ridge responds to the large Gjalp, Vatnajökull eruption of Oct. 1996. The *vertical red bar* in Nov. 1998 marks the time of the successfully stress-forecast  $M$  5 (Crampin et al. 1999, 2008). (Modified after Volti and Crampin 2003b)

swarm event in Iceland (Crampin et al. 2008) to the  $M$  9.2, 2004, Sumatra-Andaman Earthquake (SAE), where changes in SWS were recognized in Iceland at the width of the Eurasian Plate ( $\sim 10,500$  km) from Indonesia (Crampin and Gao 2012). Before SAE, ten stress-forecasts were emailed to IMO (13th Sept., 2002 to 18th Feb., 2005) updated every few months, warning of an impending large earthquake (Crampin and Gao 2012). At that time the full NLD sensitivity of SWS had not been recognized, and a  $M \approx 7$  earthquake in Iceland was stress-forecast. It was only in retrospect that it was recognized that the stress-forecasts were for the SAE (Crampin and Gao 2012).

Stress-forecasting is possible whenever SWS can be routinely monitored. Swarms of small earthquakes are generally far too scarce and irregular for routine monitoring of SWS. Only in Iceland where two transform faults of the Mid-Atlantic Ridge uniquely run onshore in SW Iceland and North-Central Iceland and provide the persistent low-level seismicity necessary for reliable routine stress-forecasting (Volti and Crampin 2003a, b).

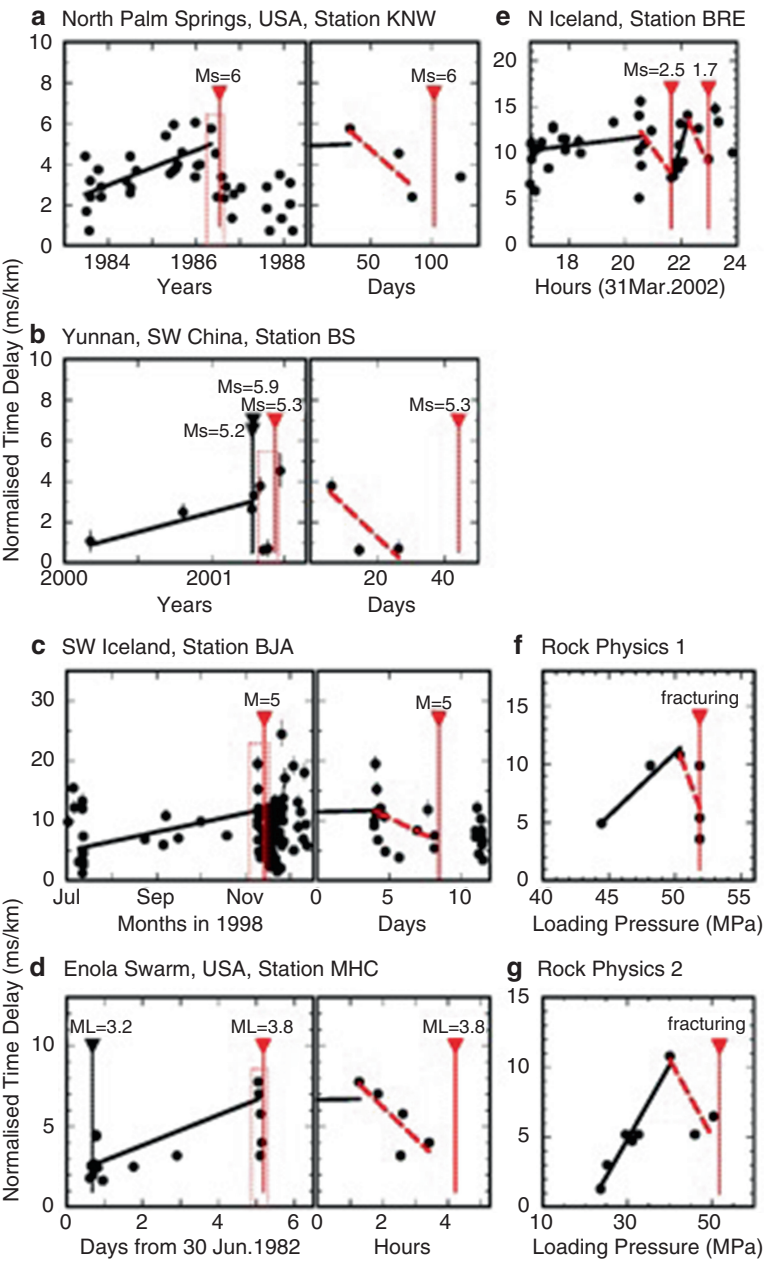


**Fig. 7** Examples of stress-accumulation and stress-relaxation in field and in laboratory. Shear-wave time delays normalized to ms/km and plotted against time before six earthquakes ranging in magnitude from  $M_s = 6$  to  $M = 1.7$  and two laboratory experiments. More complete information is in Gao and Crampin (2004)

Note that New Geophysics implies that earthquakes cannot be predicted by monitoring effects at the source. Earthquakes are singularities which lead to deterministic chaos; thus, although the source effects may on occasions be modelled explicitly, they are essentially unrepeatable as they are likely to depend critically on otherwise negligible (butterfly effect) details of initial conditions. The only mechanism for stress-forecasting/prediction is using SWS to monitor stress-accumulation and stress-relaxation in the rock surrounding the impending earthquake (or volcanic eruption) by the conventional effects of changing stress on microcrack geometry in rocks surrounding the impending source (Crampin 1999; Crampin et al. 2008). The source of the shear-waves may either be the irregular and unreliable swarms of small earthquakes, or controlled-source Stress-Monitoring Sites (SMSs) (Crampin and Gao 2016). SMSs provide a mechanism for routinely monitoring stress accumulating before impending earthquakes and volcanic eruptions so that the earthquake or eruption can be stress-forecast.

### **Appendix 3: Monitoring NLD Deformation to Stress-Forecast Impending Volcanic Eruptions**

Monitoring SWS before impending volcanic eruptions shows similar characteristic NLD deformation behaviour as that seen before earthquakes and can be similarly interpreted as stress-accumulation and stress-relaxation before the event.

Figure 8 compares stress-accumulation and stress-relaxation, in the normalized format of Fig. 7, before (a) the 2010 ash-cloud (flank) eruption of Eyjafjallajökull Volcano in SW Iceland (Liu et al. 1997) with (b) the successfully stress-forecast earthquake in Fig. 7c 90 km to the west (Gao and Crampin 2004). Both events show stress-accumulation increases, of 7 months and 4 months, respectively, and stress-relaxation decreases, of ~40 days and four days, respectively. Considering the very different geophysical processes involved, the NLD behaviour of the variations of SWS time-delays seems remarkably similar and supports the existence of New Geophysics in the reservoir rock.

### **Appendix 4: Monitoring Fluid Injection (Aka Hydraulic Fracking)**

Angerer et al. (2002) use APE to model the response of a cracked carbonate reservoir to critically high-pressure and low-pressure CO<sub>2</sub> injections (hydraulic fracking). Figure 9 shows seismograms of a multi-component 4-D (time-lapse 3-D) 3C reflection survey in Vacuum Field, New Mexico, in 1995, by the Reservoir Characterization Project (RCP), Colorado School of Mines (Roche et al. 1997).

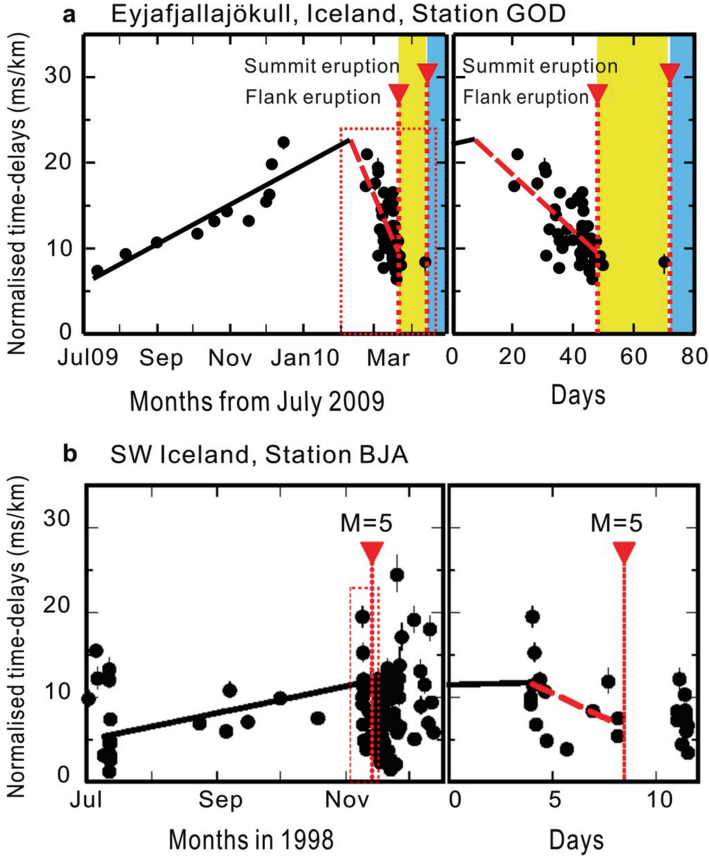


**Fig. 8** Comparison of the behaviour of shear-wave splitting before (a) a volcanic eruption and before (b) an earthquake. The eruption is the ash cloud eruption of Vatnajökull, Iceland, March 2010 and the earthquake is in SW Iceland in Fig. 7c. Both show similar stress-accumulation increases and brief stress-relaxation (crack coalescence) decreases before both eruption and earthquake occurs

The record sections headed *S1* and *S2* are in the same orthogonal azimuthal directions. In (a) the pre- $\text{CO}_2$  injection: the arrowed arrivals at the top and bottom of the target zone are at 176 ms for *S1* and 178 ms *S2* so that *S1* is the faster shear wave. In (b) the post- $\text{CO}_2$  injection, the target zone is at 204 ms for the *S1*-direction and 184 ms for *S2*. This means that the high-pore fluid pressure injection is critically high and has induced a  $90^\circ$ -flip in the orientation of the faster split shear-wave arrivals for both observed and calculated seismograms for shear waves travelling through the injection zone. Such  $90^\circ$ -flips have since been observed elsewhere in high-pressure reservoirs and near seismically active fault-planes where critically high pore-fluid pressures are encountered on all seismically active fault-planes (Crampin et al. 2002, 2004b).

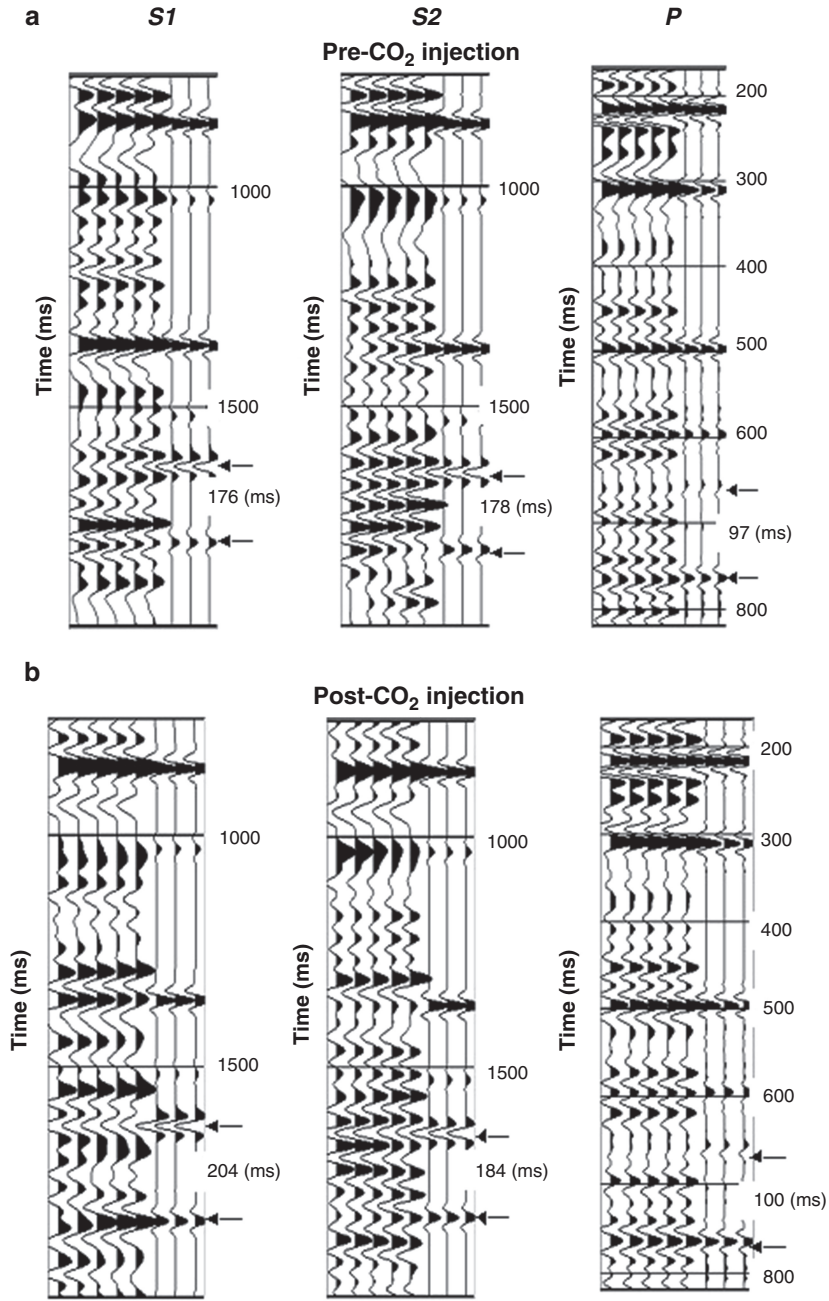


Fig. 9 (continued)

The 90°-flip was not expected, and the match of observations with APE is strong confirmation of the validity of APE and New Geophysics in crustal rock.

## References

- Ando, M., Y. Ishikawa, and H. Wada. 1980. S-wave anisotropy in the upper mantle under a volcanic area in Japan. *Nature* 286: 43–46.
- Angerer, E., S. Crampin, X.-Y. Li, and T.L. Davis. 2002. Processing, modelling, and predicting time-lapse effects of overpressured fluid-injection in a fractured reservoir. *Geophysical Journal International* 149: 267–280.
- Booth, D.C., and S. Crampin. 1985. Shear-wave polarizations on a curved wavefront at an isotropic free-surface. *Geophysical Journal of the Royal Astronomical Society* 83: 31–45.
- Crampin, S. 1981. A review of wave motion in anisotropic and cracked elastic-media. *Wave Motion* 3: 343–391.
- . 1994. The fracture criticality of crustal rocks. *Geophysical Journal International* 118: 428–438.
- . 1999. Calculable fluid-rock interactions. *Journal of the Geological Society* 156: 501–514.
- . 2003. Aligned cracks not LPO as the cause of mantle anisotropy, EGS-AGU-EUG Joint Ass., Nice, 2003. *Geophysical Research Abstract* 5: 00205; with up-dated notes in online version.
- . 2006. The New Geophysics: a new understanding of fluid-rock deformation. In *Eurock 2006: multiphysics coupling and long term behaviour in rock mechanics*, ed. A. Van Cotthem, R. Charlier, J.-F. Thimus, and J.-P. Tshibangu, 539–544. London: Taylor & Francis.
- Crampin, S., R. Evans, B. Üçer, M. Doyle, J.P. Davis, G.V. Yegorkina, and A. Miller. 1980. Observations of dilatancy-induced polarization anomalies and earthquake prediction. *Nature* 286: 874–877.
- Crampin, S., and Y. Gao. 2012. Plate-wide deformation before the Sumatra-Andaman earthquake. *Journal of Asian Earth Sciences* 46: 61–19. doi:10.1016/j.jseas.2011.1015.
- . 2013. The New Geophysics. *Terra Nova* 25: 173–180. doi:10.1111/ter.12030.
- . 2015. The physics underlying Gutenberg-Richter in the Earth and in the Moon. *Journal of Earth Science* 26: 134–139. doi:10.1007/s12583-015-0523-3.
- . 2016. Borehole Stress-Monitoring Sites (SMSs) for monitoring stress accumulation and predicting (stress-forecasting) impending earthquakes and eruptions. In *Workshop on earthquakes in North Iceland: proceedings WENI2 workshop*, Húsavík Academic Center, Iceland, in press.



**Fig. 9** (a) Pre-injection waveforms of a multi-component nearly vertical ray reflection survey near the centre of Vacuum Field, New Mexico, carbonate reservoir (Angerer et al. 2002). S1-, S2-, and P-waves are reflection sections with mutually orthogonal polarizations, where the horizontals S1, and S2, have been rotated into the split shear-wave polarizations parallel and perpendicular to the direction of maximum horizontal stress, respectively. Left-hand (LH) five traces are observed waveforms at adjacent recorders 17 m apart, and the right-hand (RH) three traces are synthetic seismograms modelled by APE to match the shear-wave and SWS arrivals. *Top* and *bottom* of injection zone for shear waves are marked by *arrows* with time-delays in ms/km. (b) Post-injection waveforms two-weeks after a high-pressure CO<sub>2</sub>-injection (hydraulic fracking). Again, the LH traces are observations and RH traces are synthetic seismograms modelled by APE with the structure from (a) and an injection pressure of 6.4 MPa (after Angerer et al. 2002)

- Crampin, S., Y. Gao, and A. De Santis. 2013. A few earthquake conundrums resolved. *Journal of Asian Earth Sciences* 62: 501–509. doi:10.1016/j.jseas.1012.10.036.
- Crampin, S., Y. Gao, and S. Peacock. 2008. Stress-forecasting (not predicting) earthquakes: a paradigm shift. *Geology* 36: 427–430.
- Crampin, S., and S.C. Kirkwood. 1981. Velocity variations in systems of anisotropic symmetry. *Journal of Geophysics* 49: 35–42.
- Crampin, S., and S. Peacock. 2005. A review of shear-wave splitting in the compliant crack-critical anisotropic Earth. *Wave Motion* 41: 59–77.
- . 2008. A review of the current understanding of shear-wave splitting and common fallacies in interpretation. *Wave Motion* 45: 675–722.
- Crampin, S., S. Peacock, Y. Gao, and S. Chastin. 2004b. The scatter of time-delays in shear-wave splitting above small earthquakes. *Geophysical Journal International* 156: 39–44.
- Crampin, S., T. Volti, S. Chastin, A. Gudmundsson, and R. Stefánsson. 2002. Indication of high pore fluid pressures in a seismically-active fault zone. *Geophysical Journal International* 151: F1–F5.
- Crampin, S., T. Volti, and R. Stefánsson. 1999. A successfully stress-forecast earthquake. *Geophysical Journal International* 138: F1–F5.
- . 2004a. Response to “A statistical evaluation of a ‘stress forecast’ earthquake” by T. Seher & I. G. Main. *Geophysical Journal International* 157: 194–199.
- Crampin, S., and S.V. Zatsepin. 1997a. Changes of strain before earthquakes: the possibility of routine monitoring of both long-term and short-term precursors. *Journal of Physics of the Earth* 45: 1–26.
- . 1997b. Modelling the compliance of crustal rock: II – response to temporal changes before earthquakes. *Geophysical Journal International* 129: 495–506.
- Gao, Y., and S. Crampin. 2004. Observations of stress relaxation before earthquakes. *Geophysical Journal International* 157: 578–582.
- Gutenberg, B., and C.F. Richter. 1956. Magnitude and energy of earthquakes. *Annali di Geofisica* 9: 1–15.
- Hao, P., Y. Gao, and S. Crampin. 2008. An expert system for measuring shear-wave splitting above small earthquakes. *Computers & Geosciences* 34: 226–234.
- Hudson, J.A. 1981. Wave speeds and attenuation of elastic waves in material containing cracks. *Geophysical Journal International* 64: 133–150.
- Liu, Y., S. Crampin, and I. Main. 1997. Shear-wave anisotropy: spatial and temporal variations in time delays at Parkfield, Central California. *Geophysical Journal International* 130: 771–785.
- Roche, S.L., T.L. Davis, and R.D. Benson. 1997. 4-D, 3-C seismic study at vacuum field, New Mexico. In *66th Annual international SEG meeting*, expanded abstracts, 886–889.
- Savage, M.K. 1999. Seismic anisotropy and mantle deformation: what have we learned from shear wave splitting? *Reviews of Geophysics* 37: 65–106.
- Silver, P.G. 1996. Seismic anisotropy beneath the continents: probing the depths of geology. *Annual Review of Earth and Planetary Sciences* 24: 385–432.
- Volti, T., and S. Crampin. 2003a. A four-year study of shear-wave splitting in Iceland: 1. Background and preliminary analysis. In *New insights into structural interpretation and modelling*, ed. D.A. Nieuwland, vol. 212, 117–133. London: Geological Society, Special Publications.
- . 2003b. A four-year study of shear-wave splitting in Iceland: 2. Temporal changes before earthquakes and volcanic eruptions. In *New insights into structural interpretation and modelling*, ed. D.A. Nieuwland, vol. 212, 135–149. London: Geological Society, Special Publications.
- Wu, J., S. Crampin, Y. Gao, P. Hao, and Y.-T. Chen. 2006. Smaller source earthquakes and improved measuring techniques allow the largest earthquakes in Iceland to be stress-forecast (with hindsight). *Geophysical Journal International* 166: 1293–1298.

Advances in Nonlinear Geosciences

Tsonis, A.A. (Ed.)

2018, XIX, 707 p. 366 illus., 263 illus. in color.,

Hardcover

ISBN: 978-3-319-58894-0